Molecular Crystals and Liquid Crystals
Publication details, including instructions for authors and subscription information:
http://www.tandfonline.com/loi/gmcl16

Homogeneous Instability in Shear Flow of Nematics—Effect of an Oblique Magnetic Field

U. D. Kini [a]
[a] Raman Research Institute, Bangalore, 560 080, India

Version of record first published: 20 Apr 2011.

To cite this article: U. D. Kini (1984): Homogeneous Instability in Shear Flow of Nematics—Effect of an Oblique Magnetic Field, Molecular Crystals and Liquid Crystals, 116:1-2, 1-19

To link to this article: http://dx.doi.org/10.1080/00268948408072492

Mol. Cryst. Liq. Cryst., 1984, Vol. 116, pp. 1–19
0026-8941/84/1162–0001/$20.00/0

Printed in the United States of America

Homogeneous Instability in Shear Flow of Nematics—Effect of an Oblique Magnetic Field

U. D. KINI

Raman Research Institute, Bangalore 560 080, India.

(*Received July 25, 1984*)

Using the continuum theory of uniaxial nematics, the homogeneous instability (HI) threshold of a flow aligning nematic (FAN) is studied as a function of magnetic field strength and field orientation when the field is applied obliquely in a plane normal to the initial orientation of the nematic director. For general orientations of the field, the HI threshold can vary in magnitude when the sign of flow is reversed. Out of the four main situations possible, shear flow is studied in some detail. Calculations are extended to a non-flow aligning nematic (NFAN) in which HI is known to be possible under the action of sufficiently strong destabilising fields. The possibility of crossover between two uncoupled modes is investigated as a function of shear rate and field orientation. The case of negative diamagnetic susceptibility anisotropy is briefly discussed.

1. INTRODUCTION

The homogeneous instability (HI) in nematic flow has been well understood on the basis of the continuum theory.[1,2] The HI was first discovered by Pieranski and Guyon[3] when they subjected a flow aligning nematic (FAN) sample to a uniform shear rate between two plates, with the director **n** initially aligned normal to the shear plane. The HI is now known to occur due to a positive feed back mechanism[3–6] caused by an anisotropic viscous coupling between the director and velocity fields. The HI threshold increases with increasing strength of a stabilising magnetic field which is applied along the initial orientation of the director. However, at sufficiently high stabilising fields, a convective or roll instability (RI) is found to be more favourable than HI.[7] This too has been satisfactorily explained[4–7] on the basis of the continuum theory. The HI threshold in plane

Poiseuille flow has been investigated experimentally by Janossy et al[8] and theoretically by Manneville and Dubois-Violette.[9] Horn et al[10] have shown that in thick, tilted samples HI can be produced by free convection which sets in under a temperature difference established between the two plates. Theoretical investigations are in good accord with experimental observations for plane Poiseuille flow and for free convection. In a recent paper, Chilingaryan et al[11] have considered a novel flow situation on the basis of the continuum theory; this is flow down an inclined plane due to gravity. They have shown that HI is possible in this flow, but experimental investigations are yet to be reported. The effect of a destabilising field which is applied along the flow or normal to the plates is straight forward for shear flow (ref. 12). In plane Poiseuille flow calculations show[12] that a cross over from the normally favourable twist mode to the splay mode is possible in the presence of a magnetic field which is applied normal to the plates. So far we have discussed only FANs.

Investigations by Pieranski and Guyon[13-15] have shown that HI is not ordinarily possible in non-flow aligning nematics (NFAN). This is due to the breakdown of the positive feed back mechanism caused by the positive viscous coefficient α_3. The shear rate actually stabilises the initial orientation of the nematic director against homogeneous perturbations. However, RI is possible at sufficiently elevated shear rates.[13-15] It can be shown on the basis of the continuum theory that HI threshold may exist in shear flow and in plane Poiseuille flow when a sufficiently strong destabilising field is applied along the flow or normal to the plates.[16] HI can in principle occur in these cases under the joint actions of stabilising shear rate and destabilising magnetic field. This calculation has been extended to the case of HI in free convection.[17]

One of the interesting configurations which have been studied in the static limit is that of the *oblique magnetic field*. Deuling et al[18] have shown that when the direction of the applied field is varied in a plane normal to the initial orientation of the director which is aligned parallel to the plates, the Freedericsz field varies continuously from the splay value (for the field normal to the plates) to the twist value (when the field is parallel to the plates). So far, the effect of such an oblique field does not seem to have been studied in the case of HI of nematics.

In this communication, the general linearised equations governing homogeneous perturbations are set up, taking into account an oblique magnetic field. In principle, four cases can be studied, viz. shear flow, plane Poiseuille flow, free convection and gravity flow. The simplest

of these, viz. shear flow is taken up for a more detailed study. For a FAN (for example MBBA), the HI shear threshold is studied as a function of the field strength and its orientation relative to the direction of flow. In the case of a NFAN (for instance HBAB) the HI field threshold is studied as a function of the applied shear rate and the field orientation. In the latter case it is found necessary to consider both the uncoupled modes and study the possibility of a cross over between them. As full viscoelastic data for nematics with negative diamagnetic susceptibility anisotropy are not available, this case is briefly discussed.

2. DIFFERENTIAL EQUATIONS BOUNDARY CONDITION AND SOLUTION

Let the initial director orientation be $\mathbf{n}_0 = (1,0,0)$ along the x axis, with the steady state field $v_{y0}(z)$ along y and a magnetic field $\mathbf{H} = (0, H_\perp \cos\psi, H_\perp \sin\psi)$ applied in the shear (yz) plane making an angle ψ with the y axis. It is sufficient to restrict attention to the range $0 \leqslant \psi \leqslant \pi$. Consider homogeneous perturbations which depend on z; the director and velocity fields become $\mathbf{n} = (1, n_y, n_z)$, $\mathbf{v} = (v_x', v_{y0}, 0)$ where n_y, n_z, v_x' are small. Time dependence is ignored in order to facilitate calculation of the non-oscillatory HI threshold. Ignoring inertial effects, the linearised torque and force equations can be written as

$$\Gamma_y = -K_1 d^2 n_z/dz^2 - \chi_a H_\perp^2 S_\psi^2 n_z + n_y\left[\eta_2\alpha_3 S(z)/\eta_1 - \chi_a H_\perp^2 S_\psi C_\psi\right] + \alpha_3 b/\eta_1 = 0 \quad (1)$$

$$\Gamma_z = K_2 d^2 n_y/dz^2 + \chi_a H_\perp^2 C_\psi^2 n_y + n_z\left[\chi_a H_\perp^2 S_\psi C_\psi - S(z)\alpha_2\right] = 0 \quad (2)$$

$$\eta_1 dv_x'/dz + n_y S(z)(\eta_1 - \eta_2) = b \quad (3)$$

where Γ is the total torque experienced by the nematic director, K_1, K_2 the splay and twist elastic constants, α_2, α_3, $\eta_1 = (\alpha_3 + \alpha_4 + \alpha_6)/2$, $\eta_2 = \alpha_4/2$ viscosity coefficients, χ_a the diamagnetic susceptibility anisotropy, b a constant equal to the viscous stress σ_{zx}' acting in a plane (zx) normal to the shear plane, $S_\psi = \sin\psi, C_\psi = \cos\psi$ and $S(z) = dv_{y0}/dz$ the applied steady state shear rate at a point z.

It is possible to treat four important cases depending upon the way in which the primary flow or shear rate is produced in the sample and

also on the boundary conditions which are satisfied by the perturbations. These are

$$\text{shear flow:} \quad v_{y0}(z) = Sz, \qquad S = \text{constant} \tag{4}$$

$$\text{free convection:} \quad v_{y0}(z) = \bar{G}(z^3 - zh^2),$$

$$S(z) = \bar{G}(3z^2 - h^2),$$

$$\bar{G} = \rho g \beta (\Delta T)(\cos\varphi)/12\eta_2 h \tag{5}$$

where ρ is the density, g the acceleration due to gravity, β the thermal expansion coefficient, ΔT the temperature difference between the plates $z = \pm h$ and φ the angle of inclination of the plates with the vertical.

plane Poiseuille flow:

$$v_{y0}(z) = p_{0,y}(z^2 - h^2)/2\eta_2, \qquad S(z) = p_{0,y}z/\eta_2 \tag{6}$$

where $p_{0,y}$ is the pressure gradient impressed along $+y$. In all the cases, the perturbations satisfy the conditions

$$n_y(\pm h) = n_z(\pm h) = v_x'(\pm h) = 0 \tag{7}$$

The fourth possibility has to be listed separately. This is the case of gravity flow:

$$v_{y0}(z) = \rho g(z + h)(3h - z)/2\eta_2, \qquad S(z) = \rho g(h - z)/\eta_2 \tag{8}$$

with the perturbations satisfying the conditions

$$n_y(-h) = n_z(-h) = v_x'(-h) = 0;$$

$$K_1 dn_z/dz + \sigma_a n_z = dn_y/dz = dv_x'/dz = 0 \qquad \text{at} \quad z = +h \tag{9}$$

Here φ is the angle of inclination of the inclined plane $z = -h$ with the horizontal, $z = +h$ is the free surface of the nematic and σ_a the surface tension anisotropy of the free surface. The nematic is thus assumed to have a thickness of $2h$ in the steady state flow down the inclined plane.

The following observations can be made from the torque and force

equations (1)–(3): Consider first a FAN. If $\psi = 0$ or $\pi/2$, the field couples directly with one director fluctuation (either twist n_y or splay n_z) and influences the other through the viscous coupling. For these two ψ values, at a given field strength $H_\perp$, if the sign of the primary flow $v_{y0}(z)$ and equivalently that of the primary shear rate $S(z)$ is reversed at all points in the sample, the equations will remain unaltered if the sign of the twist fluctuation is also reversed. Thus the threshold condition will remain unaltered or, what is the same, the *magnitude* of the shear threshold remains the same, when the direction of flow is reversed. (This is trivially valid for the field-free case.) A similar conclusion follows for the field threshold in the case of a NFAN. The magnitude of the field threshold for $+|S(z)|$ and for $-|S(z)|$ will be the same when $\psi = 0$ or $\pi/2$.

Consider now what happens when the field orientation ψ has a general value (not 0, $\pi/2$ or π). Eqs. (1) and (2) show that there is no transformation under which they remain invariant when the primary flow direction is reversed. This means that in the case of a FAN, for a given value of $H_\perp$ and orientation ψ, the threshold condition will change when the sign of $S(z)$ is reversed; in otherwords, the *magnitude* of the shear threshold will change when the direction of flow is reversed. A similar conclusion can be arrived at for a NFAN; the field threshold for a given field orientation ψ will change for the same magnitude of the shear rate when the sign of flow in the sample is reversed. As can be seen, this is a direct consequence of the field coupling to both perturbations of the director orientation. Indeed the only transformation which leaves the equations invariant is the trivial one, $\psi \to \psi + \pi$. This is the reason why it is sufficient to confine our attention to the range $0 \leqslant \psi \leqslant \pi$.

Another observation is that in shear flow and free convection, the torque and force equations can support two independent modes. The equations for plane Poiseuille flow become asymmetric for general values of ψ. Only for the two limiting values $\psi = 0$ and $\psi = \pi/2$ will the equations support two independent modes viz. the twist and splay modes.[9] The equations for gravity flow remain asymmetrical as asymmetry is built into them. It is natural that these four flows should be studied separately, as it may be difficult to generalise all results from one case to the others. In this communication, the simplest of the four cases, viz. shear flow is studied.

Eqs. (1)–(3) are solved along with Eqs. (4) and (7). The plates $z = \pm h$ are assumed to move along $\pm y$ with velocities $\pm V/2$ respectively. Then $S(z) = S = V/2h = \text{constant}$. The sign of S can be changed by reversing the sign of V. It is convenient to transform to

the variable $\xi = z/h$ whence one writes

$$d^2n_y/d\xi^2 + A_1 n_y + A_2 n_z = 0 \tag{10}$$

$$d^2n_z/d\xi^2 + A_3 n_z + A_4 n_y = A_5 b \tag{11}$$

$$dv_x'/d\xi = \left[b - Sn_y(\eta_1 - \eta_2)\right]h/\eta_1 \tag{12}$$

$$A_1 = UC_\psi^2/K_2, \quad A_2 = \left(US_\psi C_\psi - \alpha_2 Sh^2\right)/K_2, \quad A_3 = US_\psi^2/K_1,$$

$$A_4 = \left[US_\psi C_\psi - \alpha_3 Sh^2\eta_2/\eta_1\right]/K_1, \quad A_5 = \alpha_3 h^2/\eta_1 K_1, \quad U = \chi_a h^2 H_\perp^2 \tag{13}$$

$$n_y(\pm 1) = n_z(\pm 1) = v_x'(\pm 1) = 0 \tag{14}$$

Eqs. (10)–(12) support two uncoupled modes:

Mode 1: n_y, n_z even: v_x' odd; $b \neq 0$

Mode 2: n_y, n_z odd: v_x' even; $b = 0$

For Mode 1, all perturbations can be expressed with b as amplitude and it is natural to scale the quantities with b.[19] Seeking solutions of the form $\exp(iq_z\xi)$ one finds two independent solutions for the wave vector,

$$q_{z1,z2}^2 = \left[(A_1 + A_3) \pm \left\{(A_1 + A_3)^2 - 4(A_1A_3 - A_2A_4)\right\}^{1/2}\right]/2 \tag{15}$$

While q_{z1} is generally real, q_{z2} may be real or imaginary. It is straight forward to solve Eqs. (10)–(12) by this method. However, keeping in mind the numerical results it is more convenient to use a series solution method which allows a calculation of the threshold, wave vectors at threshold as also the profiles of perturbations at threshold. Following ref. 5, the dimensionless Ericksen number

$$E_r = Sh^2\left[\alpha_2\alpha_3\eta_2/(\eta_1 K_1 K_2)\right]^{1/2} \tag{16}$$

has been used to represent the destabilising effects of the imposed shear rate. The effect of the magnetic field is measured by R_m the square of the dimensionless magnetic wave vector

$$R_m = \chi_a H_\perp^2 h^2\left(K_1 C_\psi^2 + K_2 S_\psi^2\right)/K_1 K_2 \tag{17}$$

which takes the value $\pi^2/4$ at the Freedericsz transition in the static limit.[18]

3. RESULTS FOR A FAN (MBBA)

MBBA has been chosen as the model liquid representing this class. The material constants are assumed to have the following values (see ref. 5 for relevant literature): $K_1 = 6 \times 10^{-7}$ dyne, $K_2 = 3 \times 10^{-7}$ dyne, $\chi_a = 1.15 \times 10^{-7}$ cgs, $\alpha_2 = -0.775$ poise, $\eta_1 = 0.248$ poise, $\alpha_3 = -0.012$ poise, $\eta_2 = 0.416$ poise. The semisample thickness $h = 100$ μm. As Mode 2 is found to be generally unfavourable, only Mode 1 threshold will be considered. For the field $H_\perp$ which has been applied at an angle ψ, the shear rate is varied till the condition of compatibility of Eqs. (10)–(14) is satisfied. This gives the HI shear threshold S_c or equivalently the critical value E_{rc} of the Ericksen number. For the field-free case, the HI threshold is $E_{rc} = 3.01$ corresponding to $S_c = 0.10$ sec^{-1} in fair agreement with ref. 5.

Figure 1 shows the variation of E_{rc} with the strength and orientation of an oblique magnetic field. At constant $H_\perp$, E_{rc} does not vary much with ψ when $H_\perp$ is small (= 50 gauss, Fig. 1a). When $H_\perp$ is larger (= 250 gauss; this value has been chosen as it is close to the twist Freedericsz threshold) there is a marked variation of E_{rc} with ψ. The threshold is found to have extema near $\psi = 0.8$ and 2.4 ($\approx \pi/4$ and $3\pi/4$) radians. There is also a noticeable difference in the magnitude of the HI threshold E_{rc} for negative and positive shear rates at a given ψ, especially at $\psi = \pi/4$ and $3\pi/4$. It should however be noted that though $H_\perp$ is constant in Fig. 1a, R_m varies with ψ.

Fig. 1b illustrates the variation of E_{rc} with R_m at four values of ψ, for both positive and negative shear rates. Due to perfect scaling, the curves for $\psi = 0$ and $\pi/2$ coincide. For $S > 0$, at $\psi = 0, \pi/4$ and $\pi/2$, E_{rc} decreases when R_m increases from zero. When $R_m \to \pi^2/4$, corresponding to the Freedericsz threshold for the given value of ψ, E_{rc} approaches zero. But at $\psi = 3\pi/4$, E_{rc} increases continuously with R_m and shows no tendency to dip even at $R_m = \pi^2/4$. The variation of $|E_{rc}|$ for $S < 0$ is similar except that the cases $\psi = \pi/4$ and $\psi = 3\pi/4$ have to be interchanged with respect to $S > 0$. Before dealing with a possible reason for this abnormal stabilising effect of the field $H_\perp$ for certain orientations, it may be apt to examine the plots of the wave vectors q_{z1}, q_{z2}. (Figs 1c and 1d). While q_{z1} is real, q_{z2} is the modulus of the imaginary wave vector iq_{z2} (Eq. 15). For the field-free case, q_{z1}

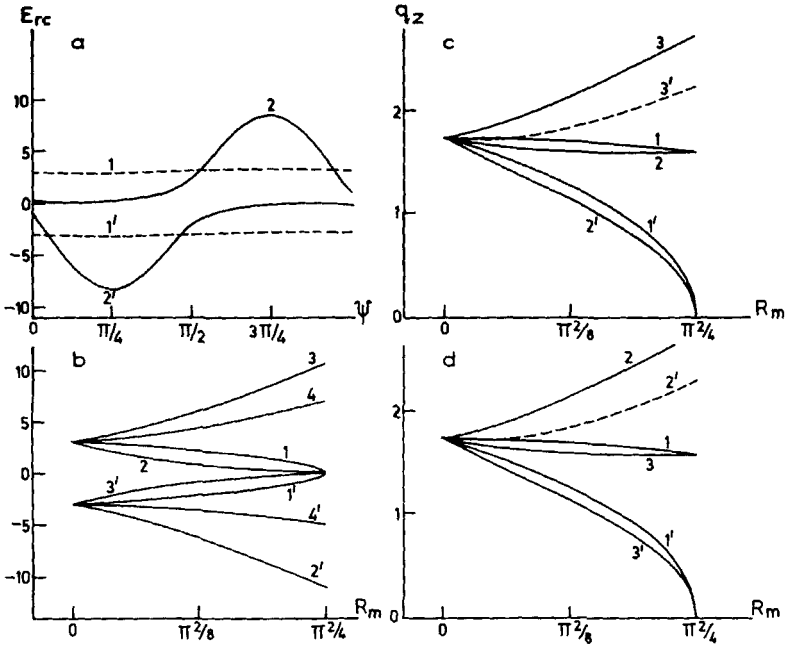

FIGURE 1 Plot of Mode 1 HI threshold E_{rc} and dimensionless wave vector q_z at threshold as functions of the oblique field $H_\perp$ (gauss) and its orientation ψ (radian). FAN. MBBA. (a) E_{rc} vs ψ at $H_\perp = (1), (1')50; (2), (2')\ 250$. (b) E_{rc} vs R_m the magnetic wave vector for different ψ. $\psi = (1), (1')\ 0, \pi/2$; (2), (2') 0.8; (3), (3') 2.4; (4) 1.8 (4') 0.3 (c) and (d) q_z vs R_m at different ψ for positive and negative shear rates. q_{z1}: $\psi = (1)\ 0, \pi/2$; (2) 0.8 (3) 2.4, q_{z2}: $\psi = (1')\ 0, \pi/2$; (2') 0.8; (3') 2.4. Note that q_{z2} is the magnitude of the imaginary wave vector.

and q_{z2} are equal $\approx 1.74 = q_0$ say. In cases where $|E_{rc}|$ decreases to zero, q_{z1} decreases from q_0 to $\pi/2$ while q_{z2} decreases to zero, as $R_m \to \pi^2/4$. At ψ values where $|E_{rc}|$ increases continuously with R_m, both the wave vectors increase from q_0. As the present calculation reflects a thought experiment in which the magnetic field $H_\perp$ is applied first and then the shear rate $|S|$ increased from zero till the HI threshold $|E_{rc}|$ is reached, values of $R_m > \pi^2/4$ are not of physical significance. Thus the curves in Fig. 1 which show a variation of the HI threshold with field strength have been truncated at $R_m = \pi^2/4$.

The HI mechanism being well understood,[4-9] the discussion in terms of the torques will be brief. The case of positive shear rate has been discussed; for $S < 0$, the explanation is similar. A fluctuation $n_z > 0$ creates a torque $\Gamma_z^{(1)} \sim A_2 n_z$ (Eq. 2). As $\alpha_2 < 0$ and $|\alpha_2| \sim 1$, $A_2 > 0$ without loss of generality. Hence $\Gamma_z^{(1)}$ gives rise to $n_y > 0$,

which in turn creates a torque $\Gamma_y^{(1)} = -A_4 n_y$. When $0 \leqslant \psi \leqslant \pi/2$, both the viscous and magnetic terms of A_4 are positive so that $\Gamma_y^{(1)} < 0$ and further increases the original fluctuation n_z in a positive feed back mechanism. The torques $\Gamma_y^{(2)} = -A_3 n_z$ and $\Gamma_z^{(2)} = A_1 n_y$ due to $H_\perp$ are always destabilising. On the other hand, when the field orientation is such that $\pi/2 \leqslant \psi \leqslant \pi$, A_4 can become negative due to the magnetic term out weighing the viscous term, as α_3 is not large. Then $\Gamma_y^{(1)} > 0$ will tend to decrease the original n_z fluctuation so that the positive feed back mechanism is no longer complete. This could explain tentatively, the anomalous stabilising effect of $H_\perp$ for certain orientations.

Fig. 2 contains normalised profiles of the perturbations at threshold, for different values of field and orientation. The profiles for negative shear rates are similar at corresponding values of field and orientation. As both E_{rc} and R_m are small, the profiles hardly show any change. Only the profile of n_z at $\psi = 2.4$ radians and $R_m = 1.85$ reflects the effects of increasing wave vector of deformation.

Before taking up the discussion of results for a NFAN, it is tempting to find out what the continuum theory predicts on the basis of the present linearised model, in the case of a FAN having negative diamagnetic anisotropy. As the full set of viscoelastic data for such a material are not available, calculations are rather speculative and

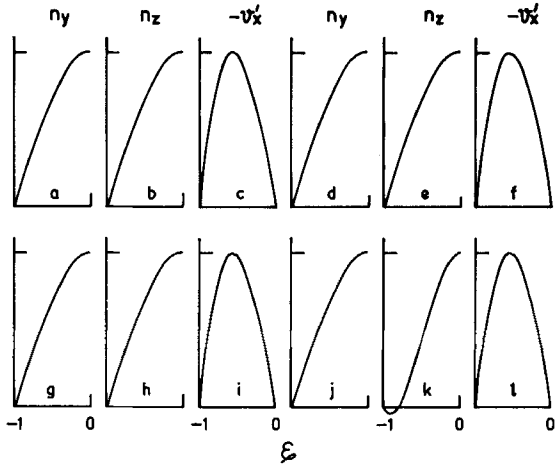

FIGURE 2 Perturbation profiles at Mode 1 threshold for $H_\perp = 250$ gauss and different field orientations ψ (radian). FAN. MBBA. $\xi = z/h$. (a), (b), (c) $\psi = 0$. $E_{rc} = 0.51$; $R_m = 2.4$. (d), (e), (f) $\psi = 0.8$; $E_{rc} = 0.31$; $R_m = 1.78$. (g), (h), (i) $\psi = \pi/2$; $E_{rc} = 2.16$; $R_m = 1.2$. (j), (k), (l) $\psi = 2.4$; $E_{rc} = 8.2$; $R_m = 1.85$.

have been performed by adopting the data for MBBA and reversing the sign of χ_a. In this case, a field $H_\parallel$ applied along the initial director orientation will have a distabilising influence. For considering the effect of $H_\parallel, H_\perp$ is equated to zero and the terms $\chi_a H_\parallel^2 n_z$ and $-\chi_a H_\parallel^2 n_y$ are added to Eqs. (1) and (2) respectively. As can be seen, the field $H_\parallel$, like the field $H_\perp$ for general orientations couples to both the director fluctuations. However the coupling is not exactly similar; $H_\parallel$ will not affect the viscous coupling in A_2 and A_4. On increasing $H_\parallel$, E_{rc} decreases and tends to zero when $H_\parallel \rightarrow$ the twist Freedericsz field (≈ 250 gauss). The decrease to zero occurs at the twist and not at the splay threshold mainly because $K_2 < K_1$ for MBBA parameters. When a field $H_\perp$ is considered, the present case is physically different from that of $\chi_a > 0$. It can be checked that when the sign of χ_a is reversed, there is no transformation which can make Eqs. (1) and (2) coincide with themselves. As R_m is negative, there is no Freedericsz threshold. Results will be stated for $S > 0$ as the results for $S < 0$ are similar. At low fields $H_\perp$, Mode 1 is always favourable. However, when $0 \leqslant \psi \leqslant \pi/2$, at sufficiently high $H_\perp$, Mode 2 has a lower threshold than Mode 1. In this ψ range, E_{rc} increases with R_m. In the ψ range $\pi/2 \leqslant \psi \leqslant \pi$, Mode 1 persists at all fields $H_\perp$; for a given ψ, E_{rc} decreases when R_m increases, tending to a lower limiting value E_0 when $H_\perp$ attains large values. The discussion for negative shear rates is similar except that one speaks of $|E_{rc}|$ and interchanges the ψ ranges with respect to the case of positive shear rate. The crossover between modes is seen to be a consequence of the unfavourable mode being associated with a higher 'dominant' wave vector q_{z1}. (ref. 5). As the HI threshold can be written as $S_c \sim Kq^2/h^2\eta$ where K and η are an average elastic constant and viscosity coefficient, a higher wave vector q implies a higher threshold. A similar crossover between modes has been predicted in another flow situation.[20]

4. RESULTS FOR A NFAN (HBAB)

HBAB has been chosen to represent this class of nematics. The material parameters have been chosen to have the following values: $K_1 = 8.44 \times 10^{-7}$ dyne, $K_2 = 4.78 \times 10^{-7}$ dyne, $\chi_a = 0.745 \times 10^{-7}$ cgs, $\alpha_2 = -0.327$ poise, $\alpha_3 = 0.0034$ poise, $\eta_1 = 0.0881$ poise, $\eta_2 = 0.1373$ poise. (see ref. 21 for relevant literature). It is well known[5-9] that HI is not possible in such a material, as the positive feed back mechanism fails due to the stabilising action of the imposed shear on the initial orientation against homogeneous perturbations. However,

taking a cue from earlier work[16,17] the effect of the destabilising field $H_\perp$ is investigated and as expected, one finds that for a given $E_r = Sh^2[-\alpha_2\alpha_3\eta_2/(\eta_1 K_1 K_2)]^{1/2}$, the HI threshold can exist when R_m exceeds a critical Value R_{mc}. Keeping in mind the possibility of crossover between the two modes,[16] both modes are investigated.

Fig. 3 illustrates the variation of R_{mc} and the threshold wave vectors as functions of the field orientation ψ at a low shear rate $|E_r| = 0.66$. One can see the marked effect of ψ on R_{mc} for $S > 0$ and $S < 0$ and also the crossover from Mode 1 to Mode 2 and then from Mode 2 to Mode 1 as ψ increases from 0 to π. The reason for this becomes more clear when the plots of the wave vectors are studied (Fig. 3c and 3d) for $S > 0$; the plots for $S < 0$ are similar and can be obtained by reflecting these curves in the q_z axis. Eq (15) shows that when $\epsilon = (A_1 - A_3)^2 + 4A_2A_4 > 0$, q_{z1} is real and q_{z2} may be real or imaginary; if $\epsilon < 0$, q_{z1} and q_{q2} are complex and conjugate to one another. The plots indicate that a wave vector changes discontinuously at a point where its nature changes from real to complex or real to imaginary and vice versa. (A plot of the absolute value of wave vector will still show discontinuity.) For Mode 2, q_{z1} is real and equal to π

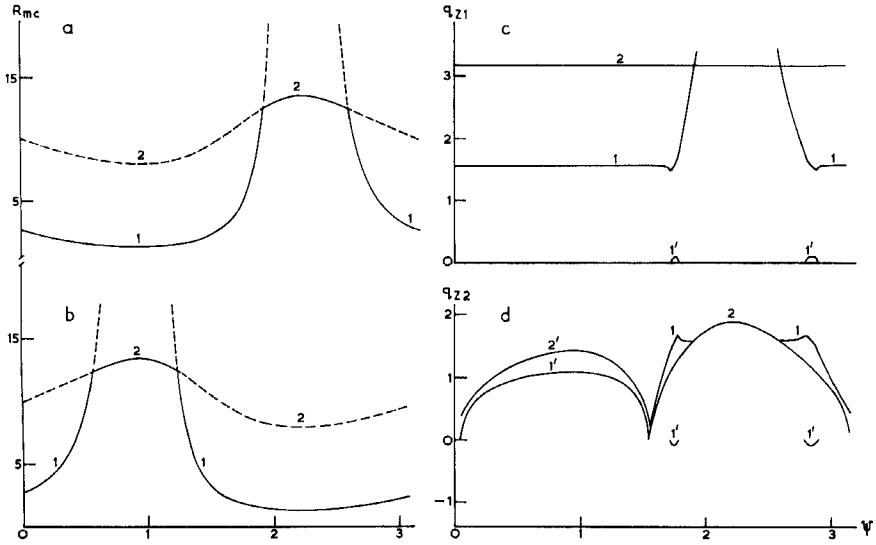

FIGURE 3 NFAN. HBAB. Plot of HI field threshold R_{mc} and threshold wave vector q_z as functions of field orientation ψ (radian) and positive and negative shear rate E_r. (a) R_{mc} vs ψ. $E_r = 0.66$. Curves 1 and 2 are for Modes 1 and 2. (b) R_{mc} vs ψ. $E_r = -0.66$. Modes 1 and 2. (c) q_{z1} vs ψ. $E_r = 0.66$. Mode 1. (1) real part (1') imaginary part. Curve 2 is for Mode 2. (d) q_{z2} vs ψ. $E_r = 0.66$. Mode 1. (1) real part (1') imaginary part. Mode 2. (2) real part (2') imaginary part.

for all ψ. For Mode 1, q_{z1} changes from real to complex at $\psi \approx 1.7$ and $\psi \approx 2.8$ radians. These approximately mark the extremities of the ψ range over which Mode 1 is not favourable. Indeed, q_{z1} for Mode 1 exceeds that of Mode 2 when $\psi \approx 1.9$; only at $\psi \approx 2.6$ radians does the Mode 1 wave vector become less than that of Mode 2. Thus q_{z1} is seen to be the dominant wave vector which controls the crossover between the two modes. Thus at a low shear rate, Mode 1 is found to be favourable over a major part of the ψ interval, viz. $0 \leqslant \psi \lesssim 1.9$ and $2.6 \lesssim \psi \leqslant \pi$, while Mode 2 has a lower threshold for $1.9 \lesssim \psi \lesssim 2.6$ radians. The plot of q_{z2} is more interesting. For both modes, q_{z2} is found to be real for small ψ, close to $\psi = 0$. When ψ increases, q_{z2} becomes purely imaginary upto $\psi \approx \pi/2$. When ψ increases further, q_{z2} for Mode 2 remains real, but q_{z2} of Mode 1 changes from real to complex more than once. There is a discontinous change associated with the change in the nature of the wave vectors.

It is straight forward to appreciate the variation of R_{mc} with ψ at a low shear rate by employing arguments based on torques as in sec. 3. Starting with a perturbation $n_z > 0$, the torque $\Gamma_z^{(1)} = A_2 n_z > 0$ gives rise to a twist $n_y > 0$ which creates the torque $\Gamma_y^{(1)} = -A_4 n_y$. As $\alpha_3 > 0$, when ψ is close to zero, $A_4 < 0$ and hence $\Gamma_y^{(1)}$ has a stabilising effect. Instability arises mainly due to the torques $-A_3 n_z$ and $A_1 n_y$ about y and z respectively. When ψ is close to $\pi/4$, the magnetic part of A_4 which is $\sim \sin 2\psi$ has maximum magnitude and can out weigh the viscous term, making $A_4 > 0$ and $\Gamma_y^{(1)} < 0$; this will tend to increase the original n_z perturbation. This could perhaps explain the dip in the field threshold for $\psi \approx \pi/4$. When ψ increases further to $\pi/2$, the magnetic part of A_4 is less dominant and the stabilising effect of the torque $\Gamma_y^{(1)}$ is reflected in the increase in R_{mc}. When ψ crosses over into the second quadrant, $\sin 2\psi$ becomes negative and A_4 remains negative. When $\psi \approx 3\pi/4$, $\sin 2\psi \approx -1$ and the stabilising effect of $\Gamma_y^{(1)}$ reaches a peak; this is responsible for the maximum in R_{mc}. Again when ψ approaches π the stabilising effect of $\Gamma_y^{(1)}$ decreases and R_{mc} again decreases.

The variation of R_{mc} with E_r for different ψ requires extensive investigation. This has been shown in Fig. 4 for a few illustrative cases. It is possible to make the following observations: The plots for $\psi = 0$ and $\pi/2$ are identical. The crossover between modes is strongly dependent on the field orientation ψ. At $\psi = 0$ and $\pi/2$, Mode 1 is more favourable at sufficiently low shear rates (Fig. 4a). At a higher shear rate E_{r1} (≈ 6) the Mode 2 threshold becomes less than that of Mode 1. Then, at a second shear rate E_{r2} (≈ 14.4) Mode 1 becomes more favourable than Mode 2 once more. It is interesting to note that

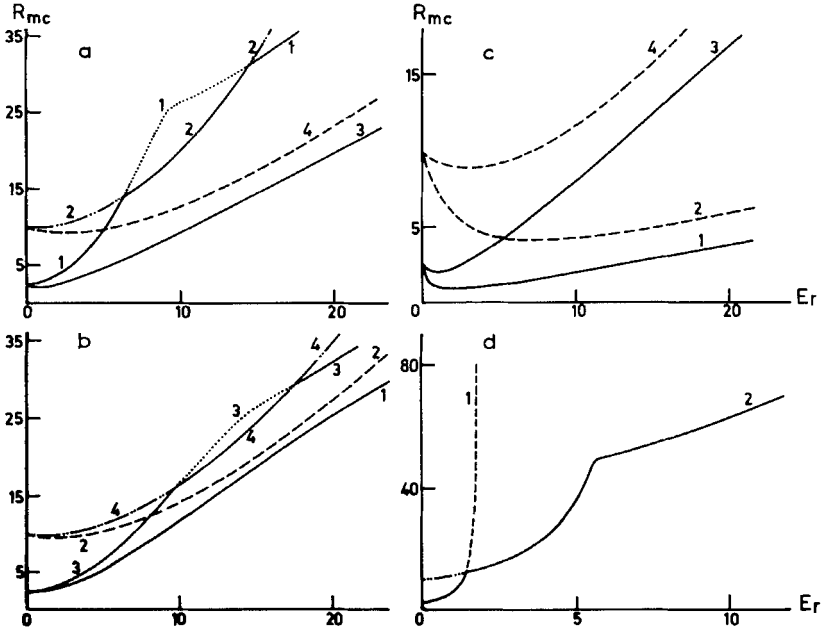

FIGURE 4 NFAN. HBAB. Plot of HI field threshold R_{mc} vs positive shear rate E_r for different field orientations ψ (radian). (a) Mode 1. ψ = (1) 0, $\pi/2$; (3) 0.1. Mode 2. ψ = (2) 0, $\pi/2$; (4) 0.1. (b) Mode 1. ψ = (1) 0.07 (3) 1.55. Mode 2. ψ = (2) 0.07 (4) 1.55. (c) Mode 1. ψ = (1) 0.8 (3) 1.5; Mode 2. ψ = (2) 0.8 (4) 1.5. (d) ψ = 1.7; Mode 1 and Mode 2 represented by curves 1 and 2.

E_{r2} corresponds to $S \approx 2.2$ sec^{-1} which is found to be the RI threshold for the HBAB parameters used here (see ref. 15). Keeping this fact in mind, parts of the curves for $E_r > 15$ may not be relevant for the present discussion. This is because, the results presented here conform to the thought experiment in which one starts with the director orientation $\mathbf{n}_0$ at a given E_r and increases $H_\perp$ from zero till the HI threshold condition is realised. If at a given E_r RI can set in, the present model will not be valid.

The influence of ψ on the cross over between the two modes can be easily seen from Fig. 4. At $\psi = 0.1, 0.07, 0.8, 1.5$ radians (Fig. 4a, 4b, 4c) Mode 1 is found to be favourable over the shear rate regime studied. When ψ is close to $\pi/2$ ($\psi = 1.55$, Fig. 4b) there are again two cross overs, but these occur at higher shear rates as compared to $\psi = \pi/2$ ($E_{r1} \approx 10$ and $E_{r2} \approx 18$). When $\pi/2 \leqslant \psi \leqslant \pi$, the Mode 1 and Mode 2 thresholds become close to one another at $\psi = 1.7$ and $\psi = 2.9$ radians (Fig. 3). The variation of the field thresholds for the two cases is found to be similar and hence only $\psi = 1.7$ has been

considered (Fig. 4d). The Mode 1 threshold increases rapidly with shear rate and Mode 2 is found to be more favourable over most of the shear rate range.

Fig. 5 exhibits the variation of the threshold wave vectors q_{z1} and q_{z2} with E_r for different ψ. The two ψ values have been chosen to represent the cases where there is crossover between the modes and where there is no crossover. At $\psi = 0$, Mode 2 has real wave vectors; the wave vectors of Mode 1 can become complex over certain shear rate ranges. The crossover of modes corresponds to that of the real part of the dominant wave vector q_{z1}. The kinks in the plots for Mode 2 are seen to occur where one wave vector reaches a multiple of π and the other starts increasing from that value to the next higher multiple of π. (Appendix I). At $\psi = 0.1$ radian, there is no crossover between the real part of the wave vector q_{z1} and Mode 1 remains more favourable throughout the shear range studied here. Fig. 6 shows some samples of perturbation profiles at threshold. The Mode 1 profiles show the influence of increasing wave vector even at $E_r \approx 15$.

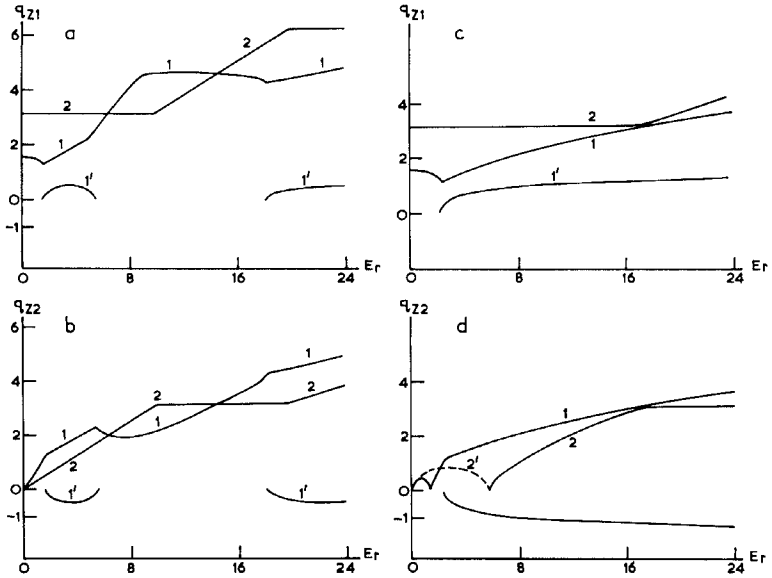

FIGURE 5 NFAN. HBAB. Plot of dimensionless wave vector at threshold, q_z vs shear rate E_r for Modes 1 and 2 at two different orientations of the oblique field. $\psi = 0$. (a) q_{z1} vs E_r. Mode 1. (1) real part (1') imaginary part. For Mode 2, q_{z1} is real. Curve 2 (b) q_{z2} vs E_r. Mode 1. (1) real part (1') imaginary part. For Mode 2, q_{z2} is real. Curve 2. $\psi = 0.1$; (c) q_{z1} vs E_r. Mode 1. (1) real part (1') imaginary part. q_{z1} is real for Mode 2. Curve 2. (d) q_{z2} vs E_r. Mode 1. (1) real part (1') imaginary part. Mode 2. (2) real part (2') imaginary part.

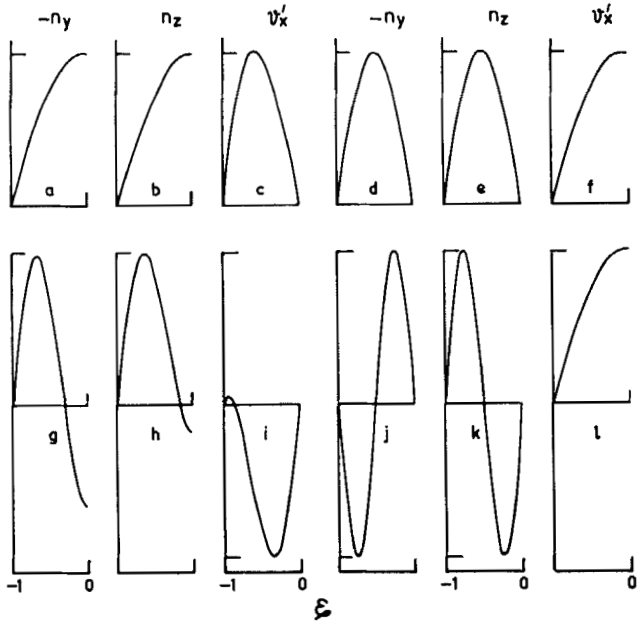

FIGURE 6 NFAN. HBAB. Perturbation profiles at HI field threshold for Modes 1 and 2. $\xi = z/h$. $E_r = 7.2$; $R_{mc} = 17.35$; $\psi = 0$; (a), (b), (c) Mode 1; (d), (e), (f) Mode 2. $R_{mc} = 15.14$. $E_r = 15.1$; $R_{mc} = 31.9$; $\psi = 0$; (g), (h), (i) Mode 1. $E_r = 13.1$; $R_{mc} = 76.9$; $\psi = 1.7$ (j), (k), (l) Mode 2.

However, the Mode 2 profiles get distorted only at much higher fields. The above descriptions have all been given for positive shear rates. The discussion for negative shear rates is similar except that the ψ ranges $0 \leqslant \psi \leqslant \pi/2$ and $\pi/2 \leqslant \psi \leqslant \pi$ have to be interchanged.

In order to understand the cross over between the modes with increasing shear rate, it is sufficient to follow the simple analysis given below. The cross over is seen mainly due to a more rapid increase of the Mode 1 threshold as compared to the Mode 2 threshold. To see this, one ignores A_5 for the moment and writes $\cos(q\xi)$ variation for the Mode 1 perturbations and $\sin(2q\xi)$ variation for the Mode 2 perturbations, with $q = \pi/2$. Eqs (10) and (11) reduce to

$$R_{mc}^{(1)} = \left[(1q)^4 + E_r^2\right]/\left[(1q)^2 + p(\psi)E_r\right]; \qquad 1 = 1,2;$$

$$p(\psi) = (\sin\psi)(\cos\psi)\zeta/(K_1\cos^2\psi + K_2\sin^2\psi); \tag{18}$$

$$\zeta = (-\eta_1\alpha_2 - \alpha_3\eta_2)(-K_1K_2/\eta_1\alpha_2\alpha_3\eta_2)^{1/2} > 0$$

as the field thresholds for Modes 1 and 2 at a given E_r. For $\psi = 0$ or $\pi/2$, $dR_{mc}^{(1)}/dE_r = 4dR_{mc}^{(2)}/dE_r$ showing that the Mode 1 threshold increases faster than the Mode 2 threshold. This is clearly a consequence of the lower elastic energy associated with the Mode 1 perturbations. A crossover between the modes cannot be ruled out. Equating the two thresholds, the E_r at which crossover is possible is found to be given by two values

$$E_{r0}(\pm) = q^2\left[5p \pm (25p^2 + 16)^{1/2}\right]/2 \tag{19}$$

one of which is positive and the other negative. For $\psi = 0$ or $\pi/2$, $p = 0$ and $E_{ro}(\pm) = \pm 2q^2 \approx \pm 5$, in fair agreement wit $Er_1 = 6$. At $\psi = \pi/4$, $E_{r0}(+) = 40$ and $E_{r0}(-) = -5$ in good agreement with the calculations. The second crossover from Mode 2 to Mode 1 which occurs for ψ close to 0 or $\pi/2$ is more complex. It is probably necessary to include the effect of A_5 in order to understand this.

Before going over to the concluding section, it may not be out of place to comment on what can be expected when the NFAN has $\chi_a < 0$. It is not known whether such a nematic fluid has been studied in the literature. Hence, for a tentative study it is enough to take the HBAB parameters with $\chi_a = -0.745 \times 10^{-7}$ cgs. As the field $H_\perp$ always stabilises the orientation, only the field $H_\parallel$ which has destabilising influence is of interest. A preliminary calculation does show a possibility of crossover between the two modes. A more detailed study will be presented in a future communication.

5. LIMITATIONS OF THE MODEL USED IN THE CALCULATIONS

In conclusion, it is necessary to critically examine the model which has been used in the present calculations. Firstly, firm anchoring has been assumed for the director orientation at the plates. Secondly, the perturbations have been assumed to be linear. This may require a more thorough investigation especially in the light of the anomalous variation of the shear threshold for MBBA at certain field orientations. One wonders whether a non-linear perturbation calculation will show a decease of E_{rc} towards zero when the field approaches the Freedericsz transition, inspite of an initial increase of the shear threshold for lower fields. Experiments should show the way in this

matter. Thirdly, the sample has been assumed to be infinite in all directions parallel to the plates. The effect of finite sample width on the occurrence of Mode 2 (which is associated with a net secondary flow) may be profound, in a real situation.

Nematic materials with $\chi_a < 0$ should form a fascinating field for study. For a proper theoretical appraisal, full data on the elastic and viscous constants of such a fluid should be available. Till then, studies like the one briefly considered in this work will remain rather tentative.

The case of steady shear flow is simple from a mathematical point of view, but may pose practical difficulties in experimental realisation, especially when an oblique magnetic field is imposed. It seems more convenient to study HI under oscillatory shear at low frequencies, as has been done in ref. 7. A theoretical study will be naturally more complicated but also more interesting, as the modal study has to consider the spatial and the temporal aspects. Theoretical studies on HI and RI under oscillatory shear and an oblique magnetic field, as also the cases of plane Poiseuille flow and gravity flow will be presented in future communications.[22]

Another situation which is convenient for study in an experiment seems to be free convection in a tilted sample. Calculations have shown that similar results for the HI threshold may be expected in this case too. This will be submitted in the near future.[23]

APPENDIX I

In this appendix, certain points pertaining to mathematical details are examined. As is clear, Mode 1 has been treated on the lines of ref. 19 by taking $b \neq 0$. This is done because of the following reasons: Firstly, modal analysis permits b to exist for Mode 1. Secondly, the effect of $v'_{x,z}$ has been absorbed from Eq. (3) into Eq. (1). With b = 0, the compatibility of Eqs. (1) and (2) does lead to a value for the Mode 1 threshold (in the case of MBBA, at zero field, $E_{rc} \approx 2.47$, close to the value 2.3 of ref. 5; the slight difference is due to the difference in the value of η_1 used.) However, with $b = 0$ if one tries to integrate Eq. (3) to find v'_x a condition connecting the material parameters and sample thickness is encountered and v'_x essentially becomes indeterminate. It also does not seem correct to retain b in Eq. (3) for determining the v'_x profile and ignore it in Eq. (1). Hence b has been retained for studying Mode 1.

Using the definition of the wave vectors from Eq. (15), the Mode 1

threshold condition can be written as

$$q_{z1}q_{z2} - S(\eta_1 - \eta_2)(X_1 q_{z1}q_{z2} + Z_1 q_{z2}\tan q_{z1} + Z_2 q_{z1}\tan q_{z2}) = 0;$$

$$X_1 = A_2A_5/\Delta, \qquad X_2 = -A_1A_5/\Delta,$$

$$\Delta = A_2A_4 - A_1A_3, \qquad \tau = q_{z1}^2 - q_{z2}^2,$$

$$Z_1 = \left[X_1(q_{z2}^2 - A_1) - X_2A_2\right]/\tau, \qquad Z_2 = \left[X_2A_2 - X_1(q_{z1}^2 - A_1)\right]/\tau \tag{A1}$$

where the possibility of one or both of the wave vectors becoming complex has to be kept in mind. For Mode 2 the threshold condition is

$$(\sin 2q_{z1})(\sin 2q_{z2})(q_{z1}^2 - q_{z2}^2) = 0 \tag{A2}$$

Here, $q_{z1} = \pi/2$ would give the Mode 1 threshold with $A_5 = 0$. Hence, $q_{z1} = m\pi$ or $q_{z2} = m\pi$ will give the Mode 2 threshold. This explains the variation of the real parts of the wave vectors for mode 2 in the case of a NFAN (sec. 4, Fig. 5). For the lowest root $q_{z1} = \pi$ or $q_{z2} = \pi$, the field threshold at a given shear rate E_r is

$$R_{mc} = (\pi^4 + E_r^2)/\left[\pi^2 + p(\psi)E_r\right] \tag{A3}$$

(see Eq. 18 for definition of p). It is more convenient to calculate the thresholds using series solution method. For Mode 1, with $n_y = \bar{n}_y + X_1$, $n_z = \bar{n}_z + X_2$,

$$(\bar{n}_y, \bar{n}_z) = \sum_{r=0}^{N} (a_r, b_r)\xi^{2r},$$

$$a_r = g_r a_0 + d_r b_0, \; b_r = e_r a_0 + z_r b_0, \; g_0 = 1 = z_0, \; e_0 = 0 = d_0 \tag{A4}$$

$$\theta_r(g_{r+1}, d_{r+1}) = -A_1(g_r, d_r) - A_2(e_r, z_r),$$

$$\theta_r(e_{r+1}, z_{r+1}) = -A_3(e_r, z_r) - A_4(g_r, d_r), \tag{A5}$$

$$\theta_r = (2r+1)(2r+2), \qquad r = 0, 1, 2, \ldots.$$

$$a_0 = \sum_{r=0}^{N} (X_2 d_r - X_1 z_r)/\varphi, \qquad b_0 = \sum_{r=0}^{N} (X_1 e_r - X_2 g_r)/\varphi, \tag{A6}$$

$$\varphi = \sum_{r=0}^{N} g_r \sum_{s=0}^{N} z_s - \sum_{r=0}^{N} e_r \sum_{s=0}^{N} d_s$$

the Mode 1 threshold is given by

$$1 - S(\eta_1 - \eta_2)\left[X_1 + \sum_{r=0}^{N} (a_0 g_r + b_0 d_r)/(2r+1)\right] = 0 \quad \text{(A7)}$$

For Mode 2, with $(n_y, n_z) = \sum_{r=0}^{N}(a_r, b_r)\xi^{2r+1}$, Eqs. (A4)–(A5) are again valid with $\theta_r = (2r+2)(2r+3)$ and the threshold condition is $\varphi = 0$, where φ is as in Eq. (A6). Though good convergence is found for $N \geqslant 25$, N has been fixed at 90 for all calculations, purely as a precautionary measure.

For MBBA, in the field free case, the function in Eq. (A7) is found to have a singularity at $|E_r| = 2.47$ ($|S| = 0.083$ sec^{-1} for $h = 100$ μm) which corresponds to the vanishing of φ. If b were taken zero, the Mode 1 threshold would simply correspond to $\varphi = 0$. In the present case, the lowest zero is found at $|E_{rc}| = 3.01$ ($S_c = 0.102$ sec^{-1}) and this has been taken as the threshold.

Acknowledgements

The author thanks Mr. V. N. K. Menon, artist, Indian Institute of Science, Bangalore, for preparing the diagrams.

References

1. P. G. De Gennes, *The Physics of Liquid Crystals* (Clarendon Press, Oxford, 1974).
2. S. Chandrasekhar, *Liquid Crystals* (Cambridge University Press, Cambridge, 1977).
3. P. Pieranski and E. Guyon, *Solid State Commun.* **13**, 435 (1973).
4. E. Guyon and P. Pieranski, *Physica* **73**, 184 (1974).
5. P. Manneville and E. Dubois-Violette, *J. Physique* **37**, 285 (1976).
6. E. Dubois-Violette, G. Durand, E. Guyon, P. Manneville and P. Pieranski, *Solid State Physics Supplement* **14** (Academic Press, 1978) 147.
7. P. Pieranski and E. Guyon, *Phys. Rev. A* **9**, 404 (1974).
8. I. Janossy, P. Pieranski and E. Guyon, *J. Physique* **37**, 1105 (1976).
9. P. Manneville and E. Dubois-Violette, *J. Physique* **37**, 1115 (1976).
10. D. Horn, E. Guyon and P. Pieranski, *Rev. Phys. Appl.* **11**, 139 (1976).
11. Yu. S. Chilingaryan, R. S. Hakopyan, N. V. Tabiryan and B. Ya. Zeldovich, *J. Physique* **45**, 413 (1984).
12. U. D. Kini, *Pramana* **10**, 143 (1978).
13. P. Pieranski and E. Guyon, *Phys. Rev. Lett.* **32**, 924 (1974).
14. P. Pieranski and E. Guyon, *Comun. Phys.* **1**, 45 (1976).
15. E. Guyon, P. Pieranski and S. A. Pikin, *J. Physique* **37**, (C1) 3(1976).
16. U. D. Kini, *Pramana* **15**, 231 (1980).
17. U. D. Kini, *Mol. Cryst. Liquid Cryst* **99**, 223 (1983).
18. H. Deuling, M. Gabay, E. Guyon and P. Pieranski, *J. Physique* **36**, 689 (1975).
19. F. M. Leslie, *J. Phys. D* **9**, 925 (1976).
20. F. M. Leslie, *Mol. Cryst. Liquid Cryst.* **37**, 335 (1976).
21. U. D. Kini, *Liquid Crystals* (S. Chandrasekhar editor, Heyden Publication 1980) 255.
22. U. D. Kini, to be published.
23. U. D. Kini, submitted to *Mol. Cryst. Liq. Cryst.*